

See discussions, stats, and author profiles for this publication at: <https://www.researchgate.net/publication/51179080>

# The Hydrogen-Bond Switch Reaction of the Blrb Bluf Domain of Rhodobacter sphaeroides

ARTICLE in THE JOURNAL OF PHYSICAL CHEMISTRY B · JUNE 2011

Impact Factor: 3.3 · DOI: 10.1021/jp201296m · Source: PubMed

CITATIONS

17

READS

30

5 AUTHORS, INCLUDING:



Tilo Mathes

ResearchGate

42 PUBLICATIONS 470 CITATIONS

SEE PROFILE



Ivo H M Van Stokkum

VU University Amsterdam

280 PUBLICATIONS 10,134 CITATIONS

SEE PROFILE



Peter Hegemann

Humboldt-Universität zu Berlin

215 PUBLICATIONS 9,407 CITATIONS

SEE PROFILE

# The Hydrogen-Bond Switch Reaction of the Blrb Bluf Domain of *Rhodobacter sphaeroides*

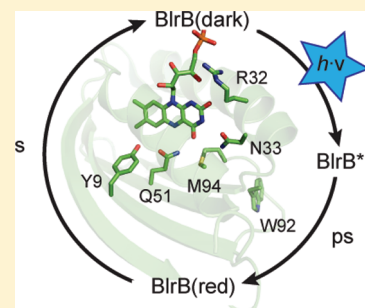
Tilo Mathes,<sup>\*,†</sup> Ivo H. M. van Stokkum,<sup>†</sup> Cosimo Bonetti,<sup>†</sup> Peter Hegemann,<sup>‡</sup> and John T. M. Kennis<sup>†</sup>

<sup>†</sup>Biophysics Group, Department of Physics and Astronomy, Faculty of Sciences, Vrije Universiteit, De Boelelaan 1081, 1081 HV, Amsterdam, The Netherlands

<sup>‡</sup>Institut für Biologie/Experimentelle Biophysik, Humboldt Universität zu Berlin, Invalidenstrasse 42, D-10115 Berlin, Germany

**S** Supporting Information

**ABSTRACT:** The BlrB protein from *Rhodobacter sphaeroides* is a small 136 amino acid photoreceptor belonging to the BLUF family of blue light receptors. It contains merely the conserved BLUF fold responsible for binding the flavin pigment and a short C-terminal extension of unknown function. We investigated the primary photoreactions of BlrB by picosecond fluorescence and transient absorption spectroscopy. After excitation of the flavin the fluorescence decays in an H/D isotope independent manner with time constants of 21 and 390 ps, indicating a BLUF characteristic heterogeneous excited state quenched by electron transfer. By transient absorption spectroscopy, we observed a rapid relaxation of a vibrationally hot excited state within 6 ps upon excitation at 400 nm. The relaxed excited state evolves biexponentially with 18 ps (27%) and 216 ps (73%) into the signaling state spectrum indicated by a growing absorptive feature at 492 nm. Additionally, a broad triplet feature is observed as residual absorbance at a delay of 5 ns, which we attribute to derive from a significant fraction of free flavin in the sample. The photochemistry of BlrB is similar to other small BLUF proteins in respect to the fast formation of the photoproduct but does not resolve any further intermediates. We compare the photoreaction with other BLUF proteins on the basis of available spectroscopic data and crystal structures. An arginine close to the C2=O carbonyl of the flavin is likely to be a key determinant for the fast electron transfer in BlrB. Additionally, the orientation of the electron-donating tyrosine in respect to the flavin might play a role in the so far unique kinetic separation of the semiquinonic intermediates in Slr1694.



## INTRODUCTION

Flavin binding photoreceptors have been extensively studied during the past 10 years.<sup>1–4</sup> The flavin cofactor differs from classical photoreceptor chromophores with its lack of photoinduced structural transitions. Similar to their well-studied role as redox and catalysis cofactors, flavin chromophores undergo light-induced redox reactions (cryptochromes),<sup>5–7</sup> covalent adduct formation (LOV domains),<sup>8–12</sup> and rearranging of hydrogen bonds.<sup>13–15</sup> BLUF (blue light sensors using FAD) domains belong to the latter group with the least chemical and structural changes and are therefore an extremely challenging field of study. Because of the ubiquitous bioavailability of flavin, BLUF photoreceptors have drawn a lot of attention as cell-type independent, noninvasive, genetically encoded, so-called optogenetic tools.<sup>16–21</sup> They are usually of modular design and contain various enzymatic domains, which are involved in second messenger (e.g., cAMP) synthesis or breakdown. The BLUF domain(s) of these proteins modulate the activity of the enzyme domains depending on the light conditions and regulate many photoprotective processes like phototaxis<sup>22,23</sup> or photosynthesis gene regulation<sup>24–26</sup> as well as biofilm formation.<sup>27,28</sup> Even though several structures of BLUF domains have been provided by X-ray crystallography and NMR spectroscopy,<sup>13,29–35</sup> key issues in the photoactivation pathway could not be addressed sufficiently since assignment of the

structures to light or dark adapted states is still under debate.<sup>13,32,33</sup>

The interaction between receptor and effector domains of these enzyme photoreceptors is also still rather unclear since only one structure of a BLUF–enzyme complex is available so far.<sup>29</sup>

The primary photoactivation mechanism of BLUF domains generally involves the flavin and at least two conserved amino acids, a tyrosine and glutamine (Y9 and Q51 in Figure 1). The tyrosine transfers an electron and most likely a proton after excitation of the flavin to yield anionic and neutral semiquinonic flavins, respectively.<sup>36</sup> Subsequently, the tyrosine/flavin radical pair recombines, and the signaling state is formed within less than 1 ns. The signaling state as observed by visible spectroscopy contains an oxidized flavin with a 10–15 nm red-shifted absorbance. Upon its ultrafast formation in <1 ns, this red-shifted state does not spectrally evolve on longer time scales.<sup>37</sup> Spectrally silent transitions that eventually affect the molecular surface likely take place on micro- to millisecond time scales.<sup>38,39</sup> From FTIR and ultrafast mid-IR absorption studies the flavin is present in a hydrogen bond switched coordination involving the glutamine side chain.<sup>40,41</sup> The amide group of the glutamine is

**Received:** February 9, 2011

**Revised:** May 10, 2011

**Published:** May 31, 2011

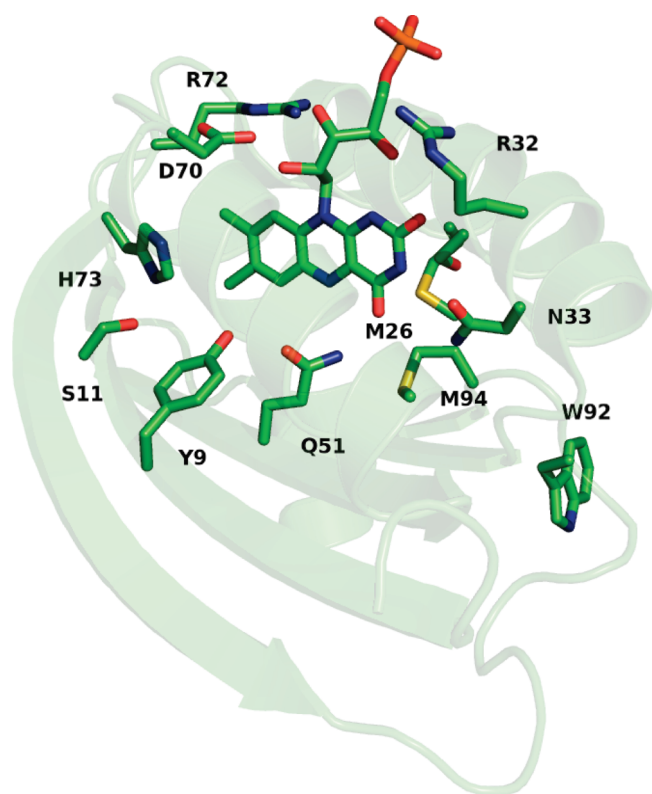


**Figure 1.** Structural features of the BlrB flavin binding pocket with the most important residues. The C-terminal helical extension is not displayed.

assumed to flip  $\sim 180^\circ$  to accommodate the experimental finding. This interpretation remains under heavy debate, since recent theoretical work suggested a transient enolization with or without flipping of the amide group, alternatively.<sup>42–45</sup> The signaling state recovers to the dark-adapted form within seconds to minutes.<sup>30,37,46,47</sup>

Many key aspects of the ultrafast hydrogen-bond switch reaction of BLUF domains remain unresolved. So far only the Slr1694 BLUF domain from *Synechocystis* sp. PCC6803 and the BLUF domain of *Rhodobacter sphaeroides* AppA were studied by ultrafast absorption and emission spectroscopy.<sup>36,37,48–51</sup> Both proteins show a highly multiexponential flavin excited-state decay which most likely reflects conformational heterogeneity of the flavin binding pocket.<sup>31,50</sup> The excited-state decay is not affected by a kinetic isotope effect when the reaction is monitored in D<sub>2</sub>O buffer, indicating electron transfer as the initial step after excitation. Intriguingly, the primary electron transfer in Slr1694 is about 10–15 times faster than in AppA<sup>36,37,40,48,50,52</sup> even though the distance of the electron-donating tyrosine to the flavin is about 0.5 Å larger.<sup>13,30,32,33</sup> Therefore, it is of high interest to study other BLUF proteins to address this obvious gap in our understanding of BLUF photochemistry. Another difference is apparent by the fact that, unlike AppA, Slr1694 kinetically resolves a number of key reactive intermediates during the ultrafast reaction. In the AppA BLUF domain, the signaling state is formed from the flavin singlet excited state without any apparent intermediates.<sup>37</sup> In Slr1694 we observe an anionic semiquinone of the flavin as the primary product of the excited-state reaction. Subsequently, formation of a neutral semiquinone is observed in an isotope-dependent kinetic.<sup>36,40</sup>

Finally, another isotope-dependent reaction to the formation of the red-shifted signaling state takes place, which is characteristic for all BLUF domains and reflects the hydrogen bond switched state.

Here we study the small BLUF protein BlrB (Figure 1) from *R. sphaeroides* by picosecond fluorescence and ultrafast visible absorption spectroscopy. BlrB is a small protein containing the BLUF domain and a short C-terminal extension similar to Slr1694 and Tll0078.<sup>30</sup> Its physiological function is unknown so far, but it is likely that the signal transduction works via protein–protein interactions similar to Slr1694.<sup>53</sup> BlrB is an ideal candidate for transient spectroscopic studies because its dark recovery of 5 s is one of the fastest among the so far characterized wild-type BLUF proteins.<sup>30</sup> Additionally, it is of high interest to study more BLUF photoreceptors in terms of electron/proton transfer kinetics to address the above-mentioned differences precisely on a molecular level.

## EXPERIMENTAL PROCEDURES

**Expression and Purification of BlrB.** *Rhodobacter sphaeroides* blrB cDNA was cloned, expressed, and purified as previously described.<sup>54</sup> Because the BLUF photochemistry is independent of the flavin identity as previously observed,<sup>55</sup> the protein was used in its heterogeneous chromophore composition after expression and purification<sup>54</sup> from *E. coli* without further pigment reconstitution with FAD. In contrast to the sample Zirak and co-workers<sup>54</sup> used, we did not remove the His-Tag.

**Streak Camera Experiments.** Time-resolved fluorescence measurements were carried out using the streak camera setup described earlier.<sup>56,57</sup> An integrated Ti:sapphire oscillator (Coherent Vitesse) produced pulses of 800 nm with 100 fs duration at 80 MHz repetition rate. This beam was directed into a regenerative amplifier (Coherent RegA) operating rate at 50 kHz. For time-resolved fluorescence experiments, the sample was diluted to an optical density (OD) at 400 nm of 0.6 per centimeter for a total volume of 8 mL. Both H<sub>2</sub>O and D<sub>2</sub>O buffers were used of 10 mM TRIS, 50 mM NaCl at a pH/pD of 8.0. To avoid multiple laser excitations on the same volume, the sample was loaded in a flow system and circulated by a peristaltic pump. A 1 mm path length flow cuvette was used. Excitation at 400 nm with a pulse energy of 10 nJ was provided by frequency doubling the output of the amplified Ti:sapphire laser system. The fluorescence was collected at 90° to the excitation path using achromatic lenses and detected through a sheet polarizer set at the magic angle (54.7°) with a Hamamatsu C5680 synchroscan streak camera and a Chromex 250IS spectrograph. The dispersed light was converted to electrons at the photocathode and time-resolved by varying the voltage applied to sweep electrodes. A microchannel-plate (MCP) was used to amplify the photocathode signal and projected to a phosphor screen where it was visualized by a CCD camera.

**Pump–Probe Spectroscopy.** Femtosecond transient absorption spectroscopy was carried out with a Ti:sapphire-based regenerative amplification system as described.<sup>58</sup> A 400 nm pump beam was obtained by frequency-doubling the output from the amplifier and attenuated to 300 nJ. Femtosecond time delays up to 5 ns between pump and probe were controlled by a delay line, and time-gated spectra at 109 delay times were recorded. The polarizations of pump and probe beams were set at the magic angle (54.7°). The instrument response function was fit to a Gaussian of 120 fs full width at half-maximum (fwhm). The samples were loaded in a flow system of 4 mL volume,

including a flow cuvette of 1 mm path length, and flowed by a peristaltic pump. Additionally, the flow cell was moved perpendicular to the probe beam by a shaking device.

**Data Analysis.** The femtosecond transient absorption data were globally analyzed using a kinetic model consisting of sequentially interconverting, evolution-associated difference spectra (EADS), i.e.,  $1 \rightarrow 2 \rightarrow 3 \rightarrow \dots$ , in which the arrows indicate successive monoexponential decays of increasing time constant, which can be regarded as the lifetime of each EADS.<sup>59</sup> The first EADS corresponds to the time-zero difference spectrum. This procedure clearly visualizes the evolution of the (excited and intermediate) states of the system. In time-resolved fluorescence measurements, an independent exponential decay scheme (sum of exponentials) is applied which produces the decay-associated spectra (DAS). It is important to note that a sequential analysis is mathematically equivalent to a parallel (sum-of-exponentials) analysis. The analysis program calculates both EADS and DADS and the time constants that follow from the analysis apply to both. In general, the EADS may well reflect mixtures of molecular states, such as may arise, for instance, from heterogeneous ground states or branching at any point in the molecular evolution.<sup>14,40,60–63</sup> The advantage of showing EADS over DADS is that the former are qualitatively and intuitively more easily interpreted in terms of which molecular species is present at what time. We stress that the sequential scheme should not *a priori* be taken literally, and the combination of different time-resolved spectroscopy information such as the transient absorption and time-resolved fluorescence with close inspection of EADS, DADS, and DAS is required to arrive at conclusions regarding the parallel, branched, or sequential nature of the spectral evolution.

To disentangle the contributions by the various molecular species in the spectral evolution, we performed a target analysis of time-resolved data. Target analysis involves the application of a compartmental model (i.e., a specific kinetic scheme) containing microscopic decay rates expressing intercompartmental transitions and may be used to test detailed hypotheses regarding the underlying kinetics. The spectrum associated with each component in a target analysis applied to difference absorption data is termed species-associated difference spectra (SADS). In contrast to the EADS, the SADS will represent the spectral signature of the pure molecular species and their kinetics after photon absorption. In this way, the reaction mechanism can be assessed in terms of discrete reaction intermediate states.

**Comparison of BLUF Protein Structures.** Molecular coordinates were obtained from the RCSB database: AppA (PDB IDs 1YRX,<sup>31</sup> 2IYG,<sup>32</sup> 2BUN<sup>13</sup>), BlrB (PDB ID 2BYC<sup>30</sup>), Slr1694 (PDB ID 2HFO<sup>33</sup>), Tll0078 (PDB ID 1XOP<sup>34</sup>). If multimers were present in the asymmetric cell, all monomers were aligned to each other using the “ligalign” script in PyMOL.<sup>64,65</sup> One representative structure was selected and aligned then with the other homologous proteins using the same procedure. All roughly aligned proteins were manually superpositioned on the isoalloxazine of the flavin cofactor of the BlrB structure.

## RESULTS

**Time-Resolved Fluorescence Spectroscopy.** The time-resolved fluorescence of the BlrB BLUF domain in both H<sub>2</sub>O and D<sub>2</sub>O buffer was recorded by means of a synchroscan streak camera with excitation at 400 nm. Global analysis of the two data sets gave decay associated spectra (DAS) with the same lifetimes

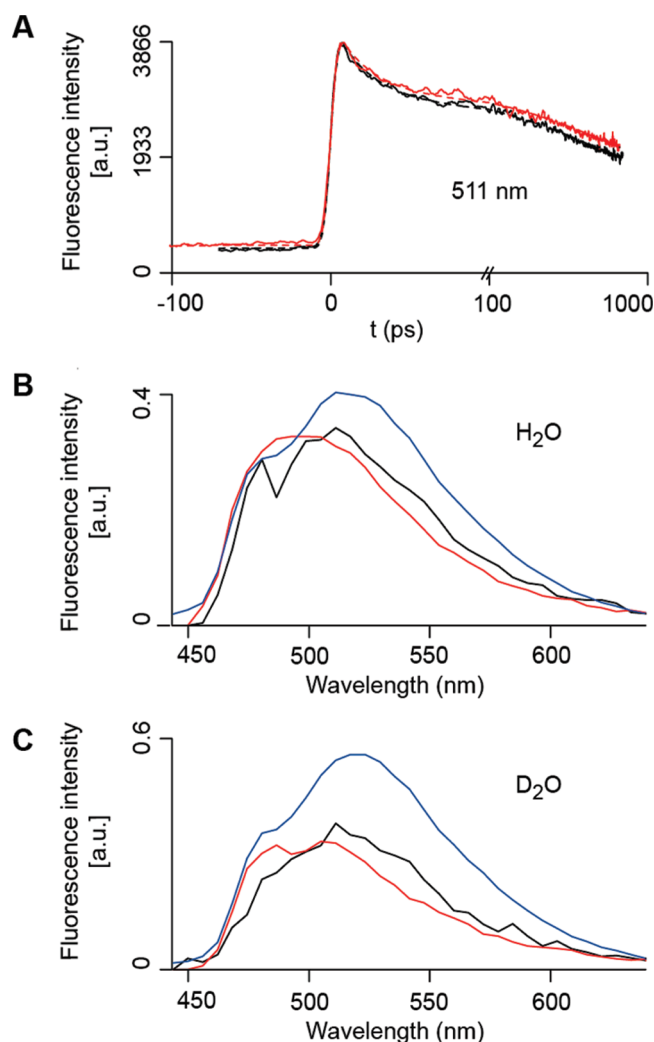


**Figure 2.** Time-resolved fluorescence of BlrB. (A) Fluorescence lifetime extracted at 511 nm (solid) along with the fitted trace (dashed). The time axis is linear until 100 ps and logarithmic after, indicated by the skewed lines. The black trace corresponds to the H<sub>2</sub>O buffered sample and red to the D<sub>2</sub>O buffered sample. The signal before time zero can be entirely attributed to a 4.4 ns decay of FAD in combination with the backsweep (after 6.5 ns) of the synchroscan streak camera system. (B) and (C) depict the decay associated spectra (DAS) of H<sub>2</sub>O and D<sub>2</sub>O sample, respectively. The time constants are 21 ps (black), 390 ps (red), and 4.4 ns (blue) for both data sets. The contribution of the free flavin was subtracted in the estimation of the relative contribution of the single DAS to the total fluorescence.

of 21 ps, 390 ps, and 4.4 ns (Figure 2B,C). The latter lifetime was fixed since it corresponds to the fluorescence lifetime of free flavin observed in previous experiments.<sup>37,40</sup> Both H<sub>2</sub>O and D<sub>2</sub>O data sets are highly similar. The black and red DAS in both data sets show a maximum at around 505 nm. A shoulder around 520 nm as observed in AppA and Slr1694 cannot be identified clearly here. Additionally, a shoulder at around 480 nm is observed, which we attribute to a photodegradation product of flavin, most likely lumichrome.<sup>54,66</sup> This shoulder is more pronounced in the DAS of the D<sub>2</sub>O sample. The two fast components are attributed to the relaxation of the BlrB excited state. In Slr1694 and in Tll0078 similarly short lifetimes were observed. The fluorescence decay in Slr1694 shows lifetimes of 6,



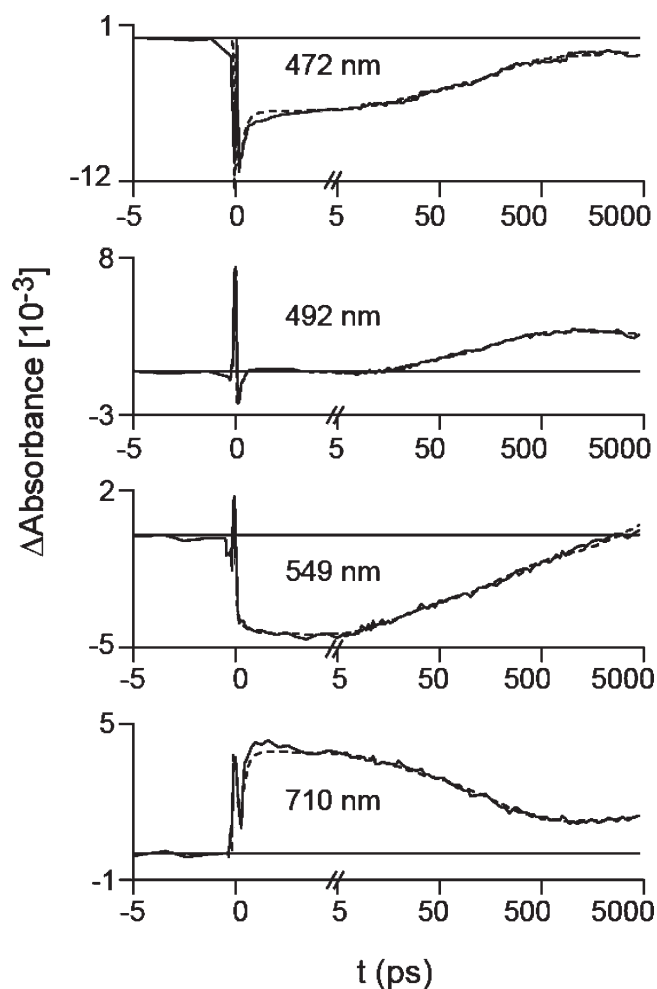


**Figure 3.** Kinetic traces at selected wavelengths extracted from the H<sub>2</sub>O data set (solid) along with the fit functions (dashed). The time scale is linear up to 5 ps and logarithmic after, indicated by the skewed lines.

26, and 92 ps with almost equal contributions and a slower component of 335 ps contributing with less than 10%.<sup>40</sup> In Tll0078 two mainly contributing lifetimes of 13.6 ps (71%) and 114 ps (27%) are observed.<sup>75</sup> A much slower fluorescence decay is observed for AppA with 620 ps as dominating species (56%) and two faster fractions decaying with 150 ps (32%) and 25 ps (10%).<sup>37,40</sup> The slower component in the BlrB data set has an emission maximum at around 520 nm, whereas the fast component seems to peak around 505 nm. According to the long lifetime and the strong fluorescence at 520 nm, a large fraction of free flavin was found to be present. The amount of flavin increased with repeated measurement (not shown) and is attributed to light induced or thermal unfolding/denaturation of the sample. The transient emission at 511 nm does not show any significant kinetic isotope effect for the samples in H<sub>2</sub>O and D<sub>2</sub>O (Figure 2A). The two traces differ only due to the fact that in the D<sub>2</sub>O sample the free flavin content is higher, thus increasing the amplitude of the slow component. The absence of a KIE is in line with previous findings on AppA and Slr1694.<sup>36,37,40</sup> A striking difference is the low stability of the flavin cofactor complex as indicated by the increasing release of the flavin during the experiment (not shown). Most likely as a consequence of the high free flavin content (~50%) of the

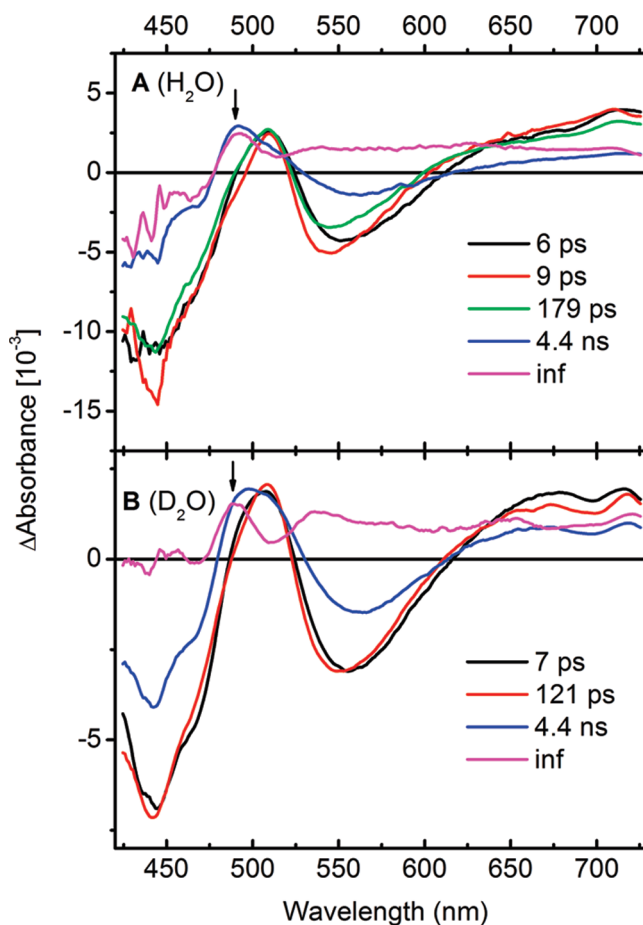


**Figure 4.** (A, B) Evolution associated difference spectra (EADS) of BlrB in H<sub>2</sub>O and D<sub>2</sub>O obtained by sequential analysis. The evolution proceeds from the black spectrum via red, green, and blue to the nondecaying magenta spectrum. In (B) only four components are necessary to describe the data sufficiently. The arrow marks an absorption feature indicative of the BLUF signaling state.

sample the data is described best with less components compared to previous experiments.

**Time-Resolved Vis Absorption Spectroscopy.** The transient data obtained by 400 nm pump–vis continuum probe spectroscopy can be sequentially (1 → 2 → 3 → 4...) modeled with four (H<sub>2</sub>O) and three (D<sub>2</sub>O) lifetimes and assigned to five/four EADS (Figure 4). The signal-to-noise ratio in the D<sub>2</sub>O data set was insufficient to estimate additional components. A fixed lifetime of 4.4 ns was assumed since we observed a high amount of free flavin in the fluorescence experiments. Time traces of selected wavelengths corresponding to ground state (GS) bleach at 472 nm, signaling state formation at 492 nm, stimulated emission (SE) at 549 nm, and excited state (ESA)/triplet absorption at 710 nm are displayed in Figure 3. Signals around  $t = 0$  ps are attributed to coherent artifact contribution generally observed in nonlinear optics.<sup>67</sup> These artifacts are taken into account by the data analysis program using a pulse follower of the instrument response. Since no significant differences were observed between H<sub>2</sub>O and D<sub>2</sub>O traces, only the H<sub>2</sub>O traces are depicted. The trace at 492 nm clearly shows the formation of the signaling state already below 50 ps. Additionally, we observe a nondecaying bleach in the trace at 472 nm. The bleach however corresponds not only

to the formation of the signaling state but also to the formation of a species absorbing at 710 nm, most likely a flavin triplet.

The black spectrum in Figure 4A represents the excited state of the flavin with a ground state (GS) bleach from 425 to 480 nm and excited-state absorption (ESA) at 510 nm and between 615 and 730 nm. Additionally, stimulated emission (SE) peaking at 551 nm is observed. Such spectral shape is typical for oxidized flavin singlet excited states.<sup>68,69</sup> Additionally, shoulders in the bleach at 445 nm are visible, which are characteristic for BLUF bound flavin absorption. The spectrum evolves into the red EADS within 6 ps, resulting in a blue shift of the stimulated emission to 546 nm without a significant loss of amplitude, which can be explained as relaxation of a vibrationally hot excited state of flavin.<sup>37,70</sup> The red spectrum then evolves into the green by another minor blue shift of the SE to 545 nm within 9 ps, indicating further excited-state relaxation. The green EADS then evolves into the blue spectrum within 179 ps. This spectrum shows the same GS bleach and similar ESA features as the previous spectra but contains a red-shifted stimulated emission at 564 nm and a new positive feature at 492 nm, which is characteristic for the red-shifted signaling state. A shoulder at  $\sim 508$  nm suggests mixing with ESA of the flavin. The SE band is about 3-fold decreased compared to the previous spectra, indicating formation of a new species. Therefore, we interpret this EADS as a mixture of free flavin because of the SE red shift and the signaling state because of the new absorptive feature at 492 nm. The spectrum evolves then with a fixed lifetime of 4.4 ns to a nondecaying species. This final shows again the same GS bleach and signaling state absorption at 492 nm. Additionally, we observe a broad absorptive feature from 500 to 730 nm which suggests the presence of a flavin triplet species. The formation of a broad absorbing species is also reflected in the 549 nm trace (Figure 3). The SE of the flavin excited state decays during the complete observation time and becomes positive only at the end. This suggests a long living excited state, most likely from free flavin.

The EADS of the D<sub>2</sub>O buffered sample (Figure 4B) are highly similar except for minor red shifts of the spectra. The hot excited state spectrum (black) shows a stimulated emission at 555 nm which evolves within 7 ps to the red spectrum with a red-shifted SE feature at 549 nm. The red spectrum then evolves within 121 ps into the blue spectrum, resulting in a loss of the SE feature by about 50%. Again, the SE is shifted to 564 nm, indicating the presence of free flavin. Additionally, a new absorptive feature at 498 nm is observed. In contrast to the H<sub>2</sub>O sample we do not observe a clear signaling state absorption, which would be expected at 492 nm. The feature of the photoproduct is occluded because the absorption is mixed with ESA of the free flavin, which is present in higher amounts in this sample. The blue spectrum evolves again with a fixed lifetime of 4.4 ns into the nondecaying spectrum (magenta). This EADS shows also the signaling state feature at  $\sim 488$  nm as well as the broad triplet absorption between 500 and 730 nm. In total, the sample behaves highly similar in both D<sub>2</sub>O and H<sub>2</sub>O buffers.

The sequential analysis is highly similar to previous analyses of the AppA BLUF domain in respect to spectral features which only represent the excited state and the signaling state,<sup>37</sup> however with different lifetimes. Therefore, we performed a similar target analysis taking into account the high amount of free flavin in the sample. This component was considered with a fixed lifetime of 4.4 ns (blue spectrum), which decays in parallel (Figure 5A). For convenience, we labeled this compartment FAD; in the sample

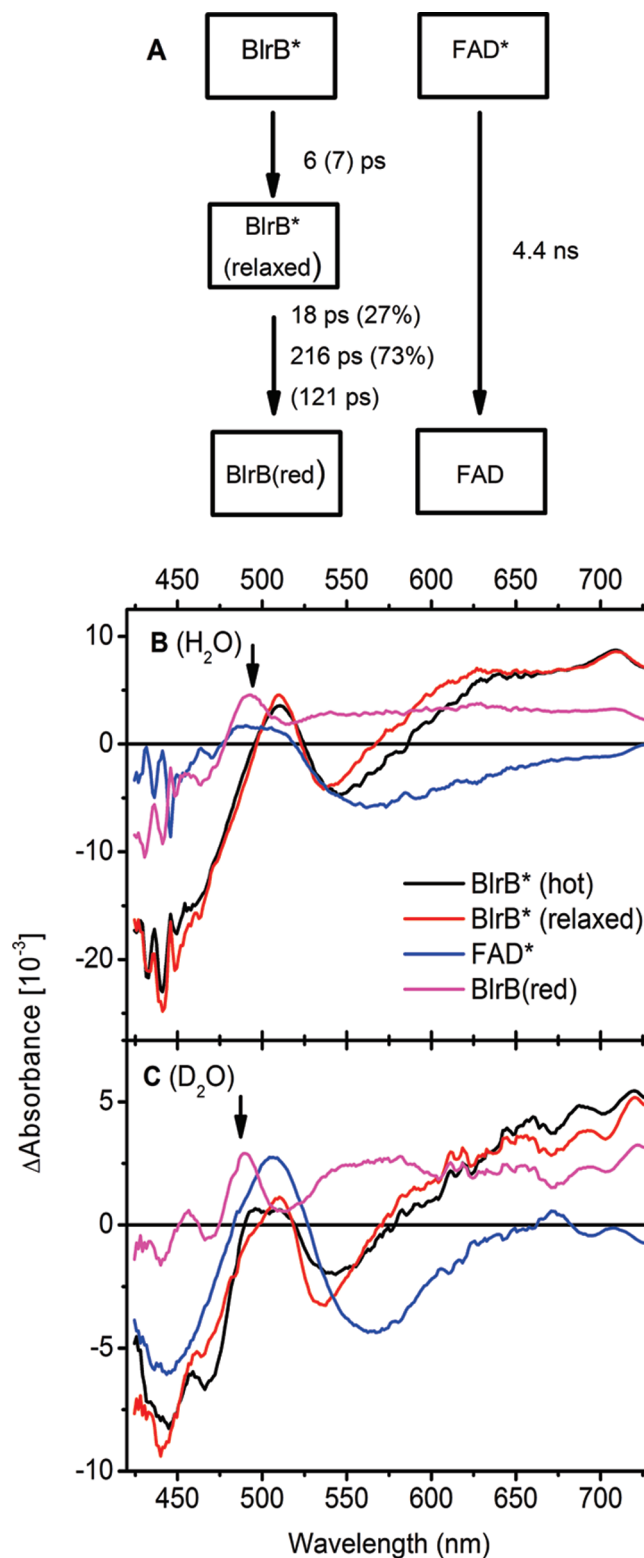


**Figure 5.** Target analysis of transient absorption data using the model displayed in (A). The time constants for D<sub>2</sub>O are displayed in parentheses. (B) and (C) show the species associated difference spectra (SADS) of H<sub>2</sub>O and D<sub>2</sub>O buffered samples, respectively. In H<sub>2</sub>O we observe a biexponential decay of the relaxed excited state (red). The SADS of the BlrB (red) species (magenta) in both experiments shows features of the signaling state as indicated by the absorption at 492 nm (arrow) as well as triplet features indicated by the broad absorption in the region between 500 and 730 nm.

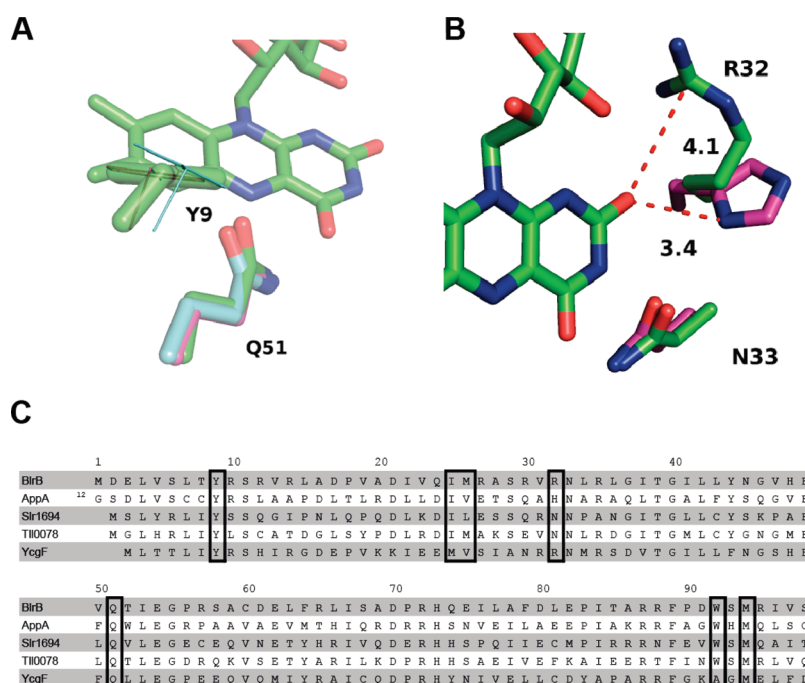


**Figure 6.** (A) shows a close-up of the relative orientation of BlrB-Y9 to the flavin overlaid with the homologous structures of AppA (magenta) and Slr1694 (cyan). The tyrosine of Slr1694 is rotated out of plane by about 35°–40°. In (B) a close-up of the region around the C2=O carbonyl of the flavin is displayed. The conserved asparagine BlrB-N33 (green) is conformationally similar to the corresponding asparagines of AppA (magenta) and Slr1694 (cyan). For the neighboring residue BlrB-R32 and the corresponding different amino acids in AppA and Slr1694 distances between the charged or polar side chain have been extracted from the structure. (C) shows an alignment of several BLUF domains that were considered in this work. Amino acid residues of interest are framed.

we have a mixture of flavins. Application of this compartmental model to the transient data set gives the species associated difference spectra (SADS) depicted in Figure 5B,C. Because of the imposed constraints of this model, the time constants differ from the ones obtained by sequential analysis.

The contribution of free flavin (50% in H<sub>2</sub>O) is again stronger in the D<sub>2</sub>O sample (60%) judged by the amplitude of stimulated emission (Figure 5B,C). The vibrationally hot excited state of BlrB (black) relaxes in both samples in about the same time with 6 and 7 ps, respectively. In the H<sub>2</sub>O sample the relaxed excited state (red) evolves biexponentially with 18 ps (27%) and 216 ps (73%); in D<sub>2</sub>O we observe a monoexponential decay of the relaxed excited state (red) with 121 ps into the long-lived photoproduct (magenta). The difference between the two data sets is most likely due to the higher flavin content in the D<sub>2</sub>O sample. The photoproduct as indicated by the new absorption at about 492 nm consists of the signaling state along with a broad triplet absorption. The fast time constant observed here corresponds nicely to the 21 ps fluorescence lifetimes obtained above. The discrepancy to the rather long-lived 390 ps component in the streak camera measurement arises most likely from the presence of free flavin, which might not be perfectly separated from the BlrB fluorescence.

FAD in aqueous solution shows heterogeneous excited-state lifetimes between picoseconds and nanoseconds, which is due to electron transfer between the isoalloxazine and adenine moieties when in a stacked conformation.<sup>71,72</sup> Here, the stimulated emission that decays in picoseconds has a maximum near 540 nm, which is associated with BLUF-bound flavins;<sup>37,40</sup> flavin in solution has a stimulated emission maximum near 560 nm.<sup>68,69</sup> We conclude that the free FAD concentration in

our sample was undetectably low. Possibly, the released FAD was hydrolyzed to FMN or photochemically degraded to lumichrome and lumiflavin forms as previously observed.<sup>66</sup> Because the adenine part of the flavin sticks out of the protein core,<sup>30</sup> it might also be possible that it is cleaved off even when the flavin is still protein bound.

The quantum yield of BlrB photoactivation as estimated by the relation between ground state bleaching in the first EADS and signaling state absorption in the last EADS is less than in Slr1694<sup>36</sup> and about the same as in AppA (24%).<sup>37</sup> If we consider the amount of free flavin (50–60%) in the sample, we can assume a signaling state quantum yield of about 48%. A previous study on a similarly produced BlrB sample showed a slightly lower quantum efficiency of about 40%.<sup>54</sup>

## DISCUSSION

BlrB belongs to the group of small BLUF proteins like Slr1694 and Tl0078, which consist mainly of the BLUF domain with a short C-terminal extension of unknown function.<sup>46</sup> AppA in contrast consists of several domains responsible for protein–protein interaction and redox sensing in the physiological context.<sup>24,73</sup> The photochemistry of the AppA–BLUF domain was, however, analyzed on both N- and C-terminally truncated constructs, which contain only the highly conserved BLUF fold. In BlrB such a functional reduction is not possible since the C-terminal extension is crucial for structural integrity.<sup>74</sup> A similar instability was observed for C-terminally truncated constructs of Slr1694 (unpublished). The primary photochemistry of BlrB is nevertheless more similar to AppA than to Slr1694. All proteins show a characteristic heterogeneity in the excited state but as in



AppA we did not observe any radical features in our data or any isotope dependent kinetics, which would hint to a proton transfer reaction. The signaling state however forms significantly faster than in AppA by a factor of 3. The analysis of the data was complicated by the fact that the protein was rather unstable under the experimental conditions, which lead to release of a high amount of free flavin. In a previous study on BlrB also a significant fraction of free flavin was determined, but to a much lesser extent (about 8%).<sup>54</sup> Using global and target analysis, we managed to extract the key features of the photoinduced reactions nevertheless. The inherent instability of the protein is hard to understand, since Slr1694 and AppA, which are highly homologous proteins, were perfectly stable under identical conditions.

Generally, it is difficult to explain the differences in the photodynamics between the various BLUF domains since we only have limited information about the structural dynamics of the protein during the ultrafast part of the photoreaction so far. Therefore, we compared the orientation of the reactive tyrosine side chain in respect to the flavin using various available crystal and NMR structures (Figure 6A), which we consider representative for the dark state. In AppA (magenta) and BlrB (green) the phenol rings of the tyrosines are coplanar but displaced by about 0.4 Å, bringing the AppA tyrosine slightly closer to the flavin. The tyrosine of Slr1694 (cyan) is slightly displaced in respect to the BlrB-Y but stays within the same range to the flavin of about 4.5 Å. The angle between the aromatic plane of the phenol ring and the isoalloxazine plane is significantly changed, as indicated by a tilt of about 35°–40° of the phenol ring in Slr1694 compared to tyrosine phenol rings in AppA and BlrB in all crystal structures. Although the phenol ring might move and rotate more or less freely within the chromophore pocket to accommodate similar orientations as observed in AppA and BlrB, which is also suggested by the single structures of the NMR structure ensemble of AppA,<sup>31</sup> this preferential relative orientation of flavin and tyrosine in the crystal might give a clue to the different dynamics/stabilities of the radical intermediates in the different BLUF domains. Minor differences in the spatial overlap of molecular orbitals (MO) of two reaction partners can have strong effects on the kinetics of the electron transfer processes. If we would further include the Tll0078 BLUF domain in Figure 6A (not shown), we would see a similarly tilted phenol ring relative to the flavin, but also a significant displacement of the side chain bringing it about 0.4 Å closer to the flavin. The ultrafast photodynamics of this protein, however, are not available for comparison at the moment. A recent fluorescent study on Tll0078 however shows a similar fast biexponential primary reaction with time constants similar to Slr1694 of about 14 and 114 ps, suggesting a similarly efficient electron transfer.<sup>75</sup>

Another key factor for the different kinetics might be the relative redox potential of the tyrosine–flavin electron transfer pair. Redox potentials are highly susceptible to the environment of the redox component and are modulated by electronic and polar interaction. In all BLUF domains the isoalloxazine ring of the flavin is surrounded mainly by well-conserved amino acid residues, some of which have been addressed by redox titration of AppA recently.<sup>76</sup> However, there is a quite variable position close to the C2=O carbonyl group, which is occupied by a moderately polar asparagine in Slr1694 (Slr-N31), a positively charged histidine according to NMR<sup>31</sup> in AppA (AppA-H44), and a positively charged arginine in BlrB (BlrB-R32) (Figure 6B). If we consider the positive charges of these amino acids to withdraw

electron density from the flavin, we would expect the flavin to be a more susceptible electron acceptor. In the structures of AppA we observe the histidine in significantly closer range to the C2=O oxygen with about 3.4 Å, in contrast to 4.1 Å for the arginine in BlrB. Therefore, one would assume that electron transfer is slower in BlrB than in AppA, which is as we have shown here not the case. Interestingly, Zirak and co-workers investigated both wild-type AppA and an AppA-H44R mutant by time-resolved fluorescence spectroscopy. They observed a 3-fold acceleration of fluorescence decay in the BlrB-like AppA-H44R mutant, similar to our findings on BlrB here.<sup>77</sup> Additionally, Zirak and co-workers observe a higher amount of free flavin studying the AppA-H44R mutant and attribute this instability to this residue, since they observe a similar behavior in BlrB.<sup>54</sup>

The occurrence of the flavin triplet in BLUF domains at these temperatures is another intriguing issue since the photoinduced electron transfer is usually fast leaving little room for the relatively slow intersystem crossing (ISC) process. Here, the majority of the flavin triplets most likely arises from the free flavin in the sample. We cannot exclude the formation of flavin triplets from the protein completely though. In AppA we observe triplet species, most likely because the electron transfer is the slowest of the so far studied BLUF domains. Additionally, we even have competing electron transfer from AppA-W104, which leads to a futile photoinduced electron transfer reaction.<sup>50,52</sup> This tryptophan is a semiconserved residue and has been found in two different conformations in crystal structures of the same protein.<sup>32,33</sup> The configurations are named W(in) and W(out) after their orientation in respect to the flavin binding pocket. A closeby conserved methionine (AppA-M106) is more or less switching positions with this tryptophane side chain creating a M(in) and M(out) conformer, respectively. In the W(in) conformation the flavin tryptophan distance is shorter, and we assume that this conformation is mainly contributing to the photoinduced electron transfer. In BLUF domains like Slr1694 we do not observe such a competing electron transfer, most likely because the Slr1694-W91-FAD distance of the W(in) conformation is significantly larger than in AppA.<sup>48</sup> For the BlrB BLUF domain we only have structural evidence for the W(out) conformation (BlrB-W92) which means that the distance is much larger and photoinduced electron transfer from this residue should be slow accordingly. However, if we consider the W(out) conformer as the dominant species in BlrB, we have the conserved methionine (BlrB-M94) in the M(in) conformation. The thioether side chain might influence the ISC rate by a heavy atom effect due to the highly polarizable sulfur atom. Additionally, BlrB contains another methionine (M26) close to the isoalloxazine ring. This feature is observed neither in Slr1694 nor in AppA, but a by one position displaced methionine in the BLUF domain of YcgF has recently been shown to influence the ISC rate in this protein.<sup>78</sup> YcgF crystal structures are not available so far but the distance between YcgF-M23 and the flavin was estimated to about 4 Å by homology models, which is similar to the distance between the sulfur atom of the reactive cysteine and the flavin in LOV domains. In the LOV2 of *Avena sativa* the heavy atom effect is assumed to be responsible for speeding up the ISC by a factor of about 2.4.<sup>68,79</sup> Since the distance between BlrB-M26 and the flavin is about 7 Å, the conserved BlrB-M94 with its shorter distance of about 4.6 Å should be considered as the predominant effector here. It should be noted that the effect needs to be unusually strong to compete with the subnanosecond electron-transfer reaction.



## CONCLUSIONS

We managed to analyze the ultrafast dynamics of another BLUF domain, BlrB, even though the protein was rather unstable under the experimental conditions. The protein shows similar features as other BLUF domains involving a heterogeneous excited state and an ultrafast formation of the signaling state. The differences in the photodynamics, especially the kinetic separation of intermediates in different BLUF domains, remain difficult to address by visible absorption spectroscopy and using static structural models. A slight difference in the main relative orientation of the tyrosine and the flavin and the resulting differences in MO overlap might account for the unique features of the Slr1694 BLUF domain. By comparison with studies on an AppA mutant, we identified an arginine residue close to the C2=O carbonyl as an effector for the faster electron transfer in BlrB in respect to AppA.

## ASSOCIATED CONTENT

**Supporting Information.** Original data of the time traces from transient absorption experiments. This material is available free of charge via the Internet at <http://pubs.acs.org>.

## AUTHOR INFORMATION

### Corresponding Author

\*E-mail [tilo.mathes.1@biologie.hu-berlin.de](mailto:tilo.mathes.1@biologie.hu-berlin.de).

## ACKNOWLEDGMENT

T.M. thanks the DFG FOR 526 for support and Gabriele Reinke for excellent technical assistance. This work was supported by the European Union through the LaserLab Europe Access Programme (T.M. and P.H.). C.B. was supported by the Life Sciences Council of The Netherlands Organization for Scientific Research (NWO-ALW). J.T.M.K. was supported by NWO-ALW through a VIDI fellowship.

## REFERENCES

- Gomelsky, M.; Klug, G. *Trends Biochem. Sci.* **2002**, *27*, 497–500.
- van der Horst, M. A.; Hellingwerf, K. J. *Acc. Chem. Res.* **2004**, *37*, 13–20.
- Möglich, A.; Yang, X.; Ayers, R. A.; Moffat, K. *Annu. Rev. Plant Biol.* **2010**, *61*, 21–47.
- Hendriks, J.; Horst, M. A.; Chua, T. K.; Pérez, M. Á.; Wilderen, L. J.; Alexandre, M. T. A.; Groot, M.-L.; Kennis, J. T. M.; Hellingwerf, K. J. In *The Purple Phototrophic Bacteria*; Advances in Photosynthesis and Respiration; Springer: Dordrecht, 2008; Vol. 28, pp 811–837.
- Langenbacher, T.; Immeln, D.; Dick, B.; Kottke, T. *J. Am. Chem. Soc.* **2009**, *131*, 14274–14280.
- Brazard, J.; Usman, A.; Lacombe, F.; Ley, C.; Martin, M. M.; Plaza, P.; Mony, L.; Heijde, M.; Zabulon, G.; Bowler, C. *J. Am. Chem. Soc.* **2010**, *132*, 4935–4945.
- Giovani, B.; Byrdin, M.; Ahmad, M.; Brettel, K. *Nat. Struct. Mol. Biol.* **2003**, *10*, 489–490.
- Christie, J. M. *Annu. Rev. Plant Biol.* **2007**, *58*, 21–45.
- Briggs, W. R. *Annu. Rev. Plant Biol.* **2009**, *61*, 1–20.
- Briggs, W. R. *J. Biomed. Sci.* **2007**, *14*, 499–504.
- Möglich, A.; Moffat, K. *J. Mol. Biol.* **2007**, *373*, 112–26.
- Kennis, J. T. M.; Alexandre, M. T. A. *Comprehensive Series in Photosciences: European Society for Photobiology*; The Royal Society for Chemistry Publishing: Cambridge, 2006; pp 287–319.
- Anderson, S.; Dragnea, V.; Masuda, S.; Ybe, J.; Moffat, K.; Bauer, C. *Biochemistry* **2005**, *44*, 7998–8005.
- Kennis, J. T. M.; Groot, M.-L. *Curr. Opin. Struct. Biol.* **2007**, *17*, 623–30.
- Masuda, S.; Hasegawa, K.; Ishii, A.; Ono, T. *Biochemistry* **2004**, *43*, 5304–5313.
- Schröder-Lang, S.; Schwärzel, M.; Seifert, R.; Strücker, T.; Kateriya, S.; Looser, J.; Watanabe, M.; Kaupp, U. B.; Hegemann, P.; Nagel, G. *Nature Methods* **2007**, *4*, 39–42.
- Stierl, M.; Stumpf, P.; Udvari, D.; Gueta, R.; Hagedorn, R.; Losi, A.; Gärtner, W.; Petereit, L.; Efetova, M.; Schwarzel, M.; Oertner, T. G.; Nagel, G.; Hegemann, P. *J. Biol. Chem.* **2010**, *286*, 1181–1188.
- Weissenberger, S.; Schultheis, C.; Liewald, J. F.; Erbguth, K.; Nagel, G.; Gottschalk, A. *J. Neurochem.* **2010**, *116*, 616–625.
- Bucher, D.; Buchner, E. *J. Neurogenet.* **2008**, *1*–5.
- Nagahama, T.; Suzuki, T.; Yoshikawa, S.; Iseki, M. *Neurosci. Res.* **2007**, *59*, 81–88.
- Ryu, M.-H.; Moskvina, O. V.; Siltberg-Liberles, J.; Gomelsky, M. *J. Biol. Chem.* **2010**, *285*, 41501–41508.
- Ntefidou, M.; Iseki, M.; Watanabe, M.; Lebert, M.; Häder, D.-P. *Plant Physiol.* **2003**, *133*, 1517–1521.
- Fiedler, B.; Börner, T.; Wilde, A. *Photochem. Photobiol.* **2005**, *81*, 1481–1488.
- Braatsch, S.; Gomelsky, M.; Kuphal, S.; Klug, G. *Mol. Microbiol.* **2002**, *45*, 827–836.
- Jäger, A.; Braatsch, S.; Haberzettl, K.; Metz, S.; Osterloh, L.; Han, Y.; Klug, G. *J. Bacteriol.* **2007**, *189*, 2274–82.
- Masuda, S.; Bauer, C. E. *Cell* **2002**, *110*, 613–623.
- Tschowri, N.; Busse, S.; Hengge, R. *Genes Dev.* **2009**, *23*, 522–34.
- Kanazawa, T.; Ren, S.; Maekawa, M.; Hasegawa, K.; Arisaka, F.; Hyodo, M.; Hayakawa, Y.; Ohta, H.; Masuda, S. *Biochemistry* **2010**, *49*, 10647–10655.
- Barends, T. R. M.; Hartmann, E.; Griese, J. J.; Beitlich, T.; Kirienko, N. V.; Ryjenkov, D. A.; Reinstein, J.; Shoeman, R. L.; Gomelsky, M.; Schlichting, I. *Nature* **2009**, *459*, 1015–1018.
- Jung, A.; Domratheva, T.; Tarutina, M.; Wu, Q.; Ko, W.-H.; Shoeman, R. L.; Gomelsky, M.; Gardner, K. H.; Schlichting, I. *Proc. Natl. Acad. Sci. U.S.A.* **2005**, *102*, 12350–5.
- Grinstead, J. S.; Hsu, S.-T. D.; Laan, W.; Bonvin, A. M. J. J.; Hellingwerf, K. J.; Boelens, R.; Kaptein, R. *ChemBioChem* **2006**, *7*, 187–93.
- Jung, A.; Reinstein, J.; Domratheva, T.; Shoeman, R. L.; Schlichting, I. *J. Mol. Biol.* **2006**, *362*, 717–32.
- Yuan, H.; Anderson, S.; Masuda, S.; Dragnea, V.; Moffat, K.; Bauer, C. *Biochemistry* **2006**, *45*, 12687–94.
- Kita, A.; Okajima, K.; Morimoto, Y.; Ikeuchi, M.; Miki, K. *J. Mol. Biol.* **2005**, *349*, 1–9.
- Wu, Q.; Gardner, K. H. *Biochemistry* **2009**, *48*, 2620–2629.
- Gauden, M.; van Stokkum, I. H. M.; Key, J. M.; Lühns, D. C.; van Grondelle, R.; Hegemann, P.; Kennis, J. T. M. *Proc. Natl. Acad. Sci. U.S.A.* **2006**, *103*, 10895–900.
- Gauden, M.; Yermenko, S.; Laan, W.; van Stokkum, I. H. M.; Ihalainen, J. A.; van Grondelle, R.; Hellingwerf, K. J.; Kennis, J. T. M. *Biochemistry* **2005**, *44*, 3653–62.
- Majerus, T.; Kottke, T.; Laan, W.; Hellingwerf, K.; Heberle, J. *ChemPhysChem* **2007**, *8*, 1787–9.
- Hazra, P.; Inoue, K.; Laan, W.; Hellingwerf, K. J.; Terazima, M. *J. Phys. Chem. B* **2008**, *112*, 1494–501.
- Bonetti, C.; Mathes, T.; van Stokkum, I. H. M.; Mullen, K. M.; Groot, M.-L.; van Grondelle, R.; Hegemann, P.; Kennis, J. T. M. *Biophys. J.* **2008**, *95*, 4790–4802.
- Masuda, S.; Hasegawa, K.; Ishii, A.; Ono, T. *Biochemistry* **2004**, *43*, 5304–13.
- Sadeghian, K.; Bocla, M.; Schütz, M. *J. Am. Chem. Soc.* **2008**, *130*, 12501–13.
- Khrenova, M. G.; Nemukhin, A. V.; Grigorenko, B. L.; Krylov, A. I.; Domratheva, T. M. *J. Chem. Theory Comput.* **2010**, *6*, 2293–2302.
- Domratheva, T.; Grigorenko, B. L.; Schlichting, I.; Nemukhin, A. V. *Biophys. J.* **2008**, *94*, 3872–9.

- (45) Khrenova, M. G.; Domratcheva, T.; Schlichting, I.; Grigorenko, B. L.; Nemukhin, A. V. *Photochem. Photobiol.* **2010**.
- (46) Okajima, K.; Yoshihara, S.; Fukushima, Y.; Geng, X.; Katayama, M.; Higashi, S.; Watanabe, M.; Sato, S.; Tabata, S.; Shibata, Y.; Itoh, S.; Ikeuchi, M. *J. Biochem.* **2005**, *137*, 741–50.
- (47) Rajagopal, S.; Key, J. M.; Purcell, E. B.; Boerema, D. J.; Moffat, K. *Photochem. Photobiol.* **2004**, *80*, 542–7.
- (48) Bonetti, C.; Stierl, M.; Mathes, T.; van Stokkum, I. H. M.; Mullen, K. M.; Cohen-Stuart, T. A.; van Grondelle, R.; Hegemann, P.; Kennis, J. T. M. *Biochemistry* **2009**, *48*, 11458–11469.
- (49) Dragnea, V.; Waagele, M.; Balascuta, S.; Bauer, C.; Dragnea, B. *Biochemistry* **2005**, *44*, 15978–85.
- (50) Gauden, M.; Grinstead, J. S.; Laan, W.; van Stokkum, I. H. M.; Avila-Pérez, M.; Toh, K. C.; Boelens, R.; Kaptein, R.; van Grondelle, R.; Hellingwerf, K. J.; Kennis, J. T. M. *Biochemistry* **2007**, *46*, 7405–15.
- (51) Stelling, A. L.; Ronayne, K. L.; Nappa, J.; Tonge, P. J.; Meech, S. R. *J. Am. Chem. Soc.* **2007**, *129*, 15556–64.
- (52) Laan, W.; Gauden, M.; Yermenko, S.; van Grondelle, R.; Kennis, J. T. M.; Hellingwerf, K. J. *Biochemistry* **2006**, *45*, 51–60.
- (53) Yuan, H.; Bauer, C. E. *Proc. Natl. Acad. Sci. U.S.A.* **2008**, *105*, 11715–9.
- (54) Zirak, P.; Penzkofer, A.; Schiereis, T.; Hegemann, P.; Jung, A.; Schlichting, I. *J. Photochem. Photobiol. B* **2006**, *83*, 180–94.
- (55) Laan, W.; Bednarz, T.; Heberle, J.; Hellingwerf, K. J. *Photochem. Photobiol. Sci.* **2004**, *3*, 1011–6.
- (56) Gobets, B.; van Stokkum, I. H. M.; Rogner, M.; Kruij, J.; Schlodder, E.; Karapetyan, N. V.; Dekker, J. P.; van Grondelle, R. *Biophys. J.* **2001**, *81*, 407–424.
- (57) Gobets, B.; Kennis, J. T. M.; Ihalainen, J. A.; Brazzoli, M.; Croce, R.; van Stokkum, I. H. M.; Bassi, R.; Dekker, J. P.; van Amerongen, H.; Fleming, G. R.; van Grondelle, R. *J. Phys. Chem. B* **2001**, *105*, 10132–10139.
- (58) Gradinaru, C. C. *Proc. Natl. Acad. Sci. U.S.A.* **2001**, *98*, 2364–2369.
- (59) van Stokkum, I. H. M.; Larsen, D. S.; van Grondelle, R. *BBA—Bioenergetics* **2004**, *1657*, 82–104.
- (60) Papagiannakis, E. *Proc. Natl. Acad. Sci. U.S.A.* **2002**, *99*, 6017–6022.
- (61) Berera, R.; van Stokkum, I. H. M.; Kodis, G.; Keirstead, A. E.; Pillai, S.; Herrero, C.; Palacios, R. E.; Vengris, M.; van Grondelle, R.; Gust, D.; Moore, T. A.; Moore, A. L.; Kennis, J. T. M. *J. Phys. Chem. B* **2007**, *111*, 6868–6877.
- (62) Bonetti, C.; Alexandre, M. T. A.; van Stokkum, I. H. M.; Hiller, R. G.; Groot, M. L.; van Grondelle, R.; Kennis, J. T. M. *Phys. Chem. Chem. Phys.* **2010**, *12*, 9256–9266.
- (63) Toh, K. C.; Stojkovic, E. A.; van Stokkum, I. H. M.; Moffat, K.; Kennis, J. T. M. *Proc. Natl. Acad. Sci. U.S.A.* **2010**, *107*, 9170–9175.
- (64) Heifets, A.; Lilien, R. H. *J. Mol. Graphics Model.* **2010**, *29*, 93–101.
- (65) Schrödinger, L. L. C. The PyMOL Molecular Graphics System, Version 1.3r1 2010.
- (66) Holzer, W.; Shirdel, J.; Zirak, P.; Penzkofer, A.; Hegemann, P.; Deutzmann, R.; Hochmuth, E. *Chem. Phys.* **2005**, *308*, 69–78.
- (67) Berera, R.; van Grondelle, R.; Kennis, J. T. M. *Photosynth. Res.* **2009**, *101*, 105–118.
- (68) Kennis, J. T. M.; Crosson, S.; Gauden, M.; van Stokkum, I. H. M.; Moffat, K.; van Grondelle, R. *Biochemistry* **2003**, *42*, 3385–3392.
- (69) Stanley, R.; MacFarlane, A. *J. Phys. Chem. A* **2000**, *104*, 6899–6906.
- (70) Wolf, M. M. N.; Schumann, C.; Gross, R.; Domratcheva, T.; Diller, R. *J. Phys. Chem. B* **2008**, *112*, 13424–13432.
- (71) van den Berg, P. A. W.; Feenstra, K. A.; Mark, A. E.; Berendsen, H. J. C.; Visser, A. J. W. G. *J. Phys. Chem. B* **2002**, *106*, 8858–8869.
- (72) Islam, S. D. M.; Susdorf, T.; Penzkofer, A.; Hegemann, P. *Chem. Phys.* **2003**, *295*, 137–149.
- (73) Han, Y.; Meyer, M. H. F.; Keusgen, M.; Klug, G. *Mol. Microbiol.* **2007**, *64*, 1090–104.
- (74) Wu, Q.; Ko, W.-H.; Gardner, K. H. *Biochemistry* **2008**, *47*, 10271–80.
- (75) Shibata, Y.; Murai, Y.; Satoh, Y.; Fukushima, Y.; Okajima, K.; Ikeuchi, M.; Itoh, S. *J. Phys. Chem. B* **2009**.
- (76) Arents, J. C.; Perez, M. A.; Hendriks, J.; Hellingwerf, K. J. *FEBS Lett.* **2011**, *585*, 167–72.
- (77) Zirak, P.; Penzkofer, A.; Hegemann, P.; Mathes, T. *Chem. Phys.* **2007**, *335*, 15–27.
- (78) Weber, S.; Schroeder, C.; Kacprzak, S.; Mathes, T.; Kowalczyk, R. M.; Essen, L.-O.; Hegemann, P.; Schleicher, E.; Bittl, R. *Photochem. Photobiol.* **2010**.
- (79) Alexandre, M. T. A.; van Grondelle, R.; Hellingwerf, K. J.; Robert, B.; Kennis, J. T. M. *Phys. Chem. Chem. Phys.* **2008**, *10*, 6693–702.